Version of Record: https://www.sciencedirect.com/science/article/pii/S0029549321003976
Manuscript_b3ea8a33436c52f86b450ff25733d436

Seismic Isolation: A Pathway to Standardized Advanced Nuclear Reactors

Sai Sharath Parsi[a], Kaivalya M. Lal[a], Benjamin D. Kosbab[b], Eric D. Ingersoll[c], Koroush Shirvan[d], and Andrew S. Whittaker[a*]

[a] University at Buffalo, The State University of New York, 212 Ketter Hall, Amherst, NY 14260, USA

[b] Simpson, Gumpertz, and Heger, Atlanta, GA, 30339, USA

[c] LucidCatalyst, Cambridge, MA, 02138, USA

[d] Massachusetts Institute of Technology, Cambridge, MA, 02139, USA

[*] Corresponding author: awhittak@buffalo.edu

Abstract

Standardizing advanced nuclear reactors is a pathway to substantially reducing their overnight capital cost and achieving parity with other power sources, including renewables and fossil fuels. The seismic load case has thwarted standardization of nuclear power plants because site-specific seismic hazard and local near-surface geology has triggered soil-structure-interaction analysis, design, equipment qualification, regulatory review, and licensing, ensuring that each build is different. To achieve standardized or site-independent certified advanced reactor designs, the impact of the seismic load case on the engineering and construction cost and time must be substantially mitigated. Seismic isolation is a mature technology that has been used for more than 30 years in non-nuclear sectors to substantially reduce earthquake demands in buildings and other infrastructure. In this paper, seismic isolation is used to enable standardization of advanced reactor designs, aimed at the complete re-use of a site-independent, certified design and repeated procurement of safety-class equipment. A pathway to standardized designs using seismic isolation is demonstrated for two fundamentally different advanced reactors: a molten salt reactor and a high temperature gas reactor. Each reactor building is equipped with three specialized pieces of safety-class equipment, namely, a reactor vessel, a steam generator, and a control rod drive mechanism housing that is attached to the reactor head. Analysis is performed per ASCE and ASME standards to design the buildings and the equipment for two base conditions: conventional (fixed base) and base isolated. The impact of the seismic load case is characterized for the reinforced concrete walls in the buildings and for the equipment, measured using vessel wall thickness and horizontal accelerations. The analysis results show that the fixed-base buildings, designed for a site of low seismic hazard (peak ground acceleration, PGA = 0.15 g) could be constructed at a site of much greater seismic hazard (PGA = 0.7 g) if seismic base isolation is employed. Importantly, the scope of the site-specific analysis, design, and qualification would be limited to the seismic isolators and the isolated substructure, drastically reducing plant-specific engineering, review, and licensing, and time to construction start. Regulatory challenges and opportunities with standardized reactor designs are identified.

1. Introduction

Recent studies have made clear the pivotal role of nuclear energy to deliver clean, affordable, and reliable electricity and meet the Paris Agreement climate goals of limiting the increase in global temperature and reach net zero carbon emissions by 2050 (e.g., Buongiorno *et al.* (2018); IAEA (2020a); Ingersoll and Gogan (2020)). This outcome will only be possible if the overnight capital cost (OCC) and levelized cost of energy of advanced nuclear reactors are on par with or lower than other energy sources, including renewable sources such as solar and wind. ETI (2020) reported the total capital cost of recent nuclear construction in the United States to be approximately $12,000/kWe (in 2017 USD), which must be reduced

to between $2,500 and $3,500 (in 2020 USD) to be commercially viable (Ingersoll *et al.*, 2020). The high OCC can be traced to a number of sources, including the seismic load case, which ensures that no two plants at different sites are identical. Standardized designs of reactor buildings and equipment, with site-specific seismic hazard analysis and geotechnical investigations but minimal site-specific analysis, design, and regulatory review, might be the only pathway to cost-competitive nuclear energy in the United States.

The seismic load case has thwarted, albeit not alone, the deployment of standardized nuclear power plants (NPPs) in the United States. Near-surface geology and seismic hazard are never identical at two NPP sites, requiring site-specific soil-structure-interaction analysis, design, equipment qualification, regulatory review, licensing, and construction. Site-independent certified NPP designs in the United States (e.g., GE ABWR, KHNP APR1400, WEC AP1000), none of which include base isolation, represent a step towards standardization but a) incur a seismic penalty in the baseline design, and b) require site-specific engineering, regulatory review, and licensing to demonstrate that the certified capacity is not exceeded.

Seismic isolation mitigates the effect of the seismic load case on design and its use could enable a rapid transition to the construction of standardized advanced reactors. Seismic isolation has been applied to many types of civil infrastructure, including mission-critical buildings, bridges, liquid natural gas tanks, and offshore oil and gas platforms over the past 30 years in the United States and abroad, and was first studied for application to advanced reactors in the late 1980s and early 1990s (e.g., Tajirian *et al.* (1989); Tajirian (1992); Tajirian and Patel (1993)). A few large light water reactors were base isolated in France (Cruas) and South Africa (Koeberg) in the 1980s (Whittaker *et al*. 2018), enabling the re-use of a design at two sites of moderately higher seismic hazard.

The conventional implementation of seismic isolation involves installation of isolators (or bearings) at the base of the building or structure per the sketch of Figure 1a, which is a cross section through a sample base-isolated reactor building, wherein the basemat is cast atop seismic isolators that are supported in turn by reinforced concrete pedestals and a foundation. Possible seismic isolators and damping devices (termed protective systems) are shown in Figure 1b (left to right: spherical sliding bearing, lead-rubber bearing, spring-based bearing, uniaxial fluid-viscous damper, and 3D pot damper, courtesy of Earthquake Protection Systems, Dynamic Isolation Systems, GERB, Taylor Devices, and GERB, respectively). The low damping rubber bearing is identical to the lead-rubber bearing except the central lead core is not included. The dashed green rectangle around the reactor building and above the isolation system identifies a standardized reactor building and components housed therein.

A standardized reactor building could host an advanced reactor from one nuclear supplier or advanced reactors of a given type and power rating from different suppliers. The latter would represent a paradigm shift in practice, where each reactor building is designed for a specific reactor type and power rating. The safety-related equipment, exclusive of that attached to the reactor head (e.g., reactor vessel auxiliary cooling system and heat exchangers) could be either reactor-supplier specific or common for reactors of a given type and power rating.

An alternate protective systems implementation for a nuclear facility, to be considered where base isolation is not practical, is to isolate structures, systems, components, and safety-class equipment at their supports inside the facility. The conventional implementation of seismic (base) isolation will enable standardized plants (i.e., building and equipment) and that is the focus of this paper. The alternate implementation would enable standardized structures, systems, components, and safety-class equipment but may not deliver the needed cost reductions for commercially viable advanced reactors.

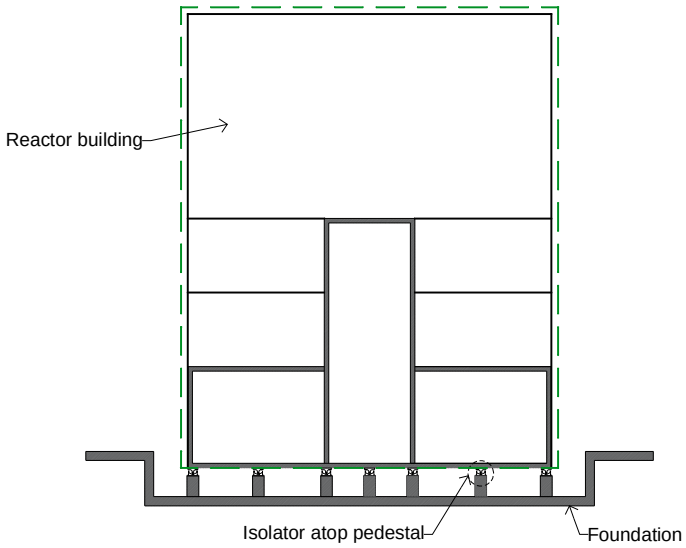

a) seismic base-isolated reactor building

b) seismic isolators and dampers

Figure 1. Seismically isolated reactor building

Although seismic isolation has been shown (e.g., Tajirian (1992); Tajirian and Patel (1993), Huang *et al.*, (2008; 2009; 2011a; 2011b), Bolisetti *et al.* (2016), Kumar *et al.*, (2017a; 2017b), Yu *et al.* (2018)) to reduce seismic demands on structures, systems, and components by factors of up to 10, and seismic risk by orders of magnitude, it has not yet been applied to nuclear power plants in the United States. The use of base isolation in the nuclear industry in the United States has been stymied by 1) few new builds, 2) a lack of technical guidance and standards, and 3) minimal quantitative information on the costs and benefits associated with base isolation.

Projects funded between 2008 and 2018 by the US Department of Energy (DOE) and the US Nuclear Regulatory Commission (NRC) provided the technical underpinnings for building-level seismic isolation of US nuclear facilities, including chapters in ASCE/SEI 4-16 (ASCE, 2017b) and ASCE/SEI 43-19 (ASCE, 2021), and three contractor reports published by the NRC: NUREG/CR-7253 (Kammerer *et al.*, 2019), NUREG/CR-7254 (Kumar *et al.*, 2019a), and NUREG/CR-7255 (Kumar *et al.*, 2019b). Journal articles, conference papers, and other technical reports support and complement the standards and guidance, with many identified in Whittaker *et al.* (2018). Information on the costs and benefits of seismic base isolation has been assembled (Lal *et al.* (2020; 2021)), with the necessary reductions in OCC for commercially viable advanced reactors being linked to standardized plants.

The remainder of this paper builds the technical case for standardized plants, made possible by building-level seismic isolation. Two advanced reactors were chosen as archetypes: a Molten Salt Reactor (MSR) and a High Temperature Gas Reactor (HTGR). These reactors are fundamentally different in many regards,

including power output (approximately 1000 MWe for the MSR and 80 MWe for the HTGR), pressure vessel design (low pressure for the MSR and high pressure for the HTGR), location and mounting of safety-class equipment, building and equipment geometry, and power density. *Generic* designs for these two reactor buildings and their safety-class equipment were developed in consultation with subject matter experts at TerraPower (MSR) and X-energy (HTGR). Each reactor building was populated with three pieces of safety-related equipment: a reactor vessel (RV), a steam generator (SG), and a control-rod drive mechanism (CRDM) housing. Numerical models of the reactor buildings with the safety-class equipment were developed and analyzed for earthquake shaking at sites of low, moderate, high, and very high seismic hazard. Each reactor building was analyzed assuming both a fixed-base and base-isolated conditions.

Section 2 describes the two example reactor buildings and the assumed safety-class equipment. Section 3 introduces the seismic hazard at the four sites. Section 4 presents preliminary designs of the two reactor buildings and the equipment. Numerical modeling and details of the response-history analysis are presented in Section 5. The impact of the seismic load case on the fixed-base buildings is described in Section 6. Section 7 presents analysis results for the base-isolated reactor buildings. Section 8 summarizes the paper, identifies key outcomes, and makes closing remarks. Appendix A introduces equipment-level seismic isolation systems, to complement the discussion in the body of the paper on the use of building-level isolation for standardizing advanced reactors.

2. Reactor buildings and safety-class equipment

The generic MSR building considered herein is a reinforced concrete (RC) structure with plan dimensions of 90 m $\times$ 60 m. The overall height is 32 m and a central wall divides the building into two compartments. The first compartment (#1) is 40 m long and houses the reactor vessel. The second compartment (#2) is 50 m long and houses four steam generators. The roof framing in both compartments are two-way slabs supported by a two-way grid of reinforced concrete beams. The perimeter walls and the central dividing wall are laterally supported by 4 m long buttresses at 10 m on center. The buttresses increase the lateral stiffness of the building and restrain out-of-plane movement of the tall walls. Figure 2 is an isometric view of the building. Figure 3 presents a top view and cross section of the building.

Compartment #1 includes a suspended RC slab that is supported by a grid of walls, 8 m above the basemat. The reactor vessel is supported at its head, at the level of the suspended floor slab. The vessel is 6 m tall including a dome-shaped base, with an inner diameter of 5 m. A 7.5 m diameter cylindrical RC structure encloses and supports the reactor vessel. A CRDM housing is attached to the top of the reactor head (see Figure 3b) as a representative head-mounted oscillator. Although a reactor head will support numerous pieces of cantilevered equipment, a representative 150-mm diameter oscillator, 2.5 m tall, with a 12 mm wall thickness, and a frequency of 22 Hz was considered here. Compartment #2 houses four steam generators, which are equally spaced at 10 m and centered between the buttresses, as shown in Figure 3a. Each 3 m diameter steam generator is 14 m tall, supported at its base on a steel frame and laterally braced at its top to the central wall and the adjacent buttresses (see Figure 3b).

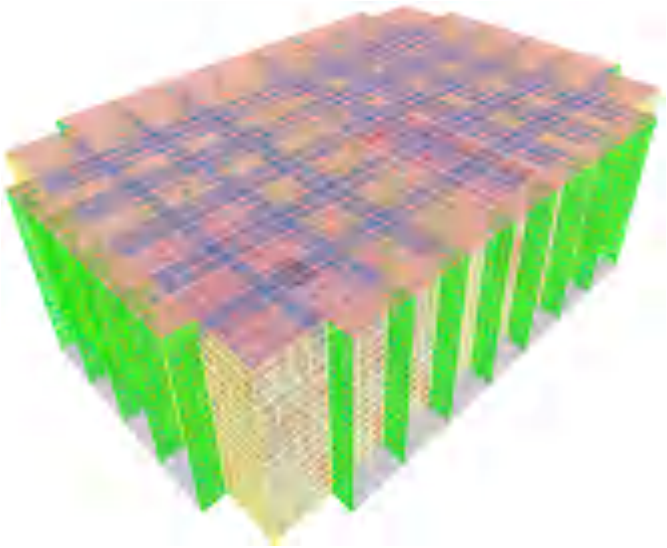

Figure 2. Isometric view of the MSR building

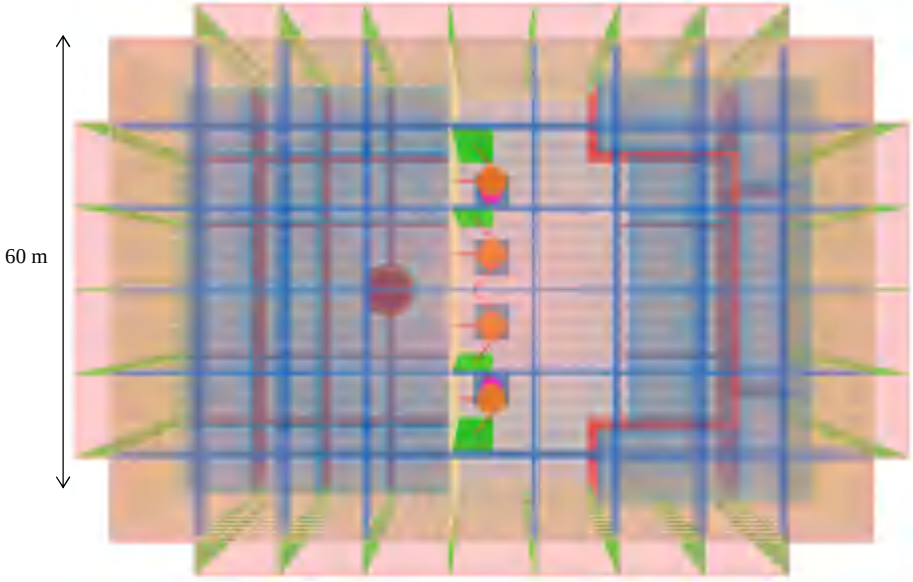

a) top view

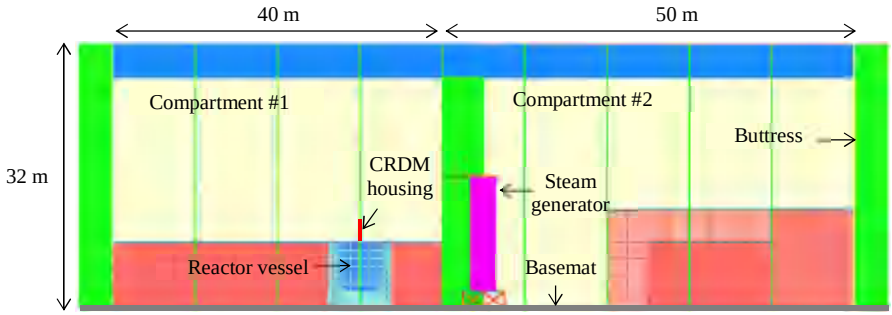

b) cross section

Figure 3. Top view and cross section of the MSR building

The generic HTGR building is a multi-story RC structure. The building is 34 m tall with plan dimensions of 24 m × 20 m. Figure 4a presents an isometric view of the building. The building includes two reinforced concrete citadels, one enclosing the reactor vessel and the other enclosing the steam generator. The citadel enclosing the reactor vessel extends from the basemat to the roof. The citadel enclosing the steam generator extends from the basemat to an elevation of 24 m.

The HTGR pressure vessel is 13 m tall with an inner diameter of 4.5 m. The vessel is supported at its base, at an elevation of 12 m, as shown in Figure 4b. The steam generator is a 14.5 m tall cylindrical vessel with an inner diameter of 3.5 m. It is supported at two-thirds of its height above its base, and at the same level as the reactor vessel. Four mounts (see green zones in Figure 4c) are extended from the steam generator to provide gravity support to the vessel on the adjacent floor slab. Similar to the MSR building, a single 250-mm diameter, 3.5-m tall CRDM housing, with a 16 mm wall thickness, is cantilevered from the top of the reactor head; its fundamental frequency is 18 Hz.

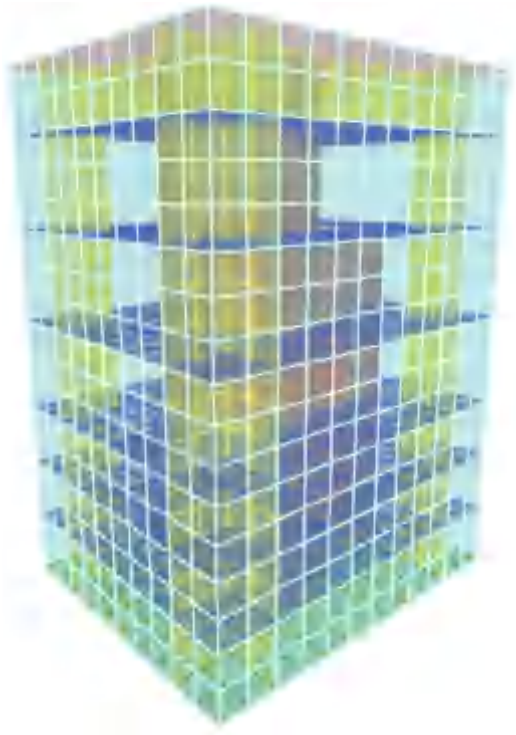

a) isometric view

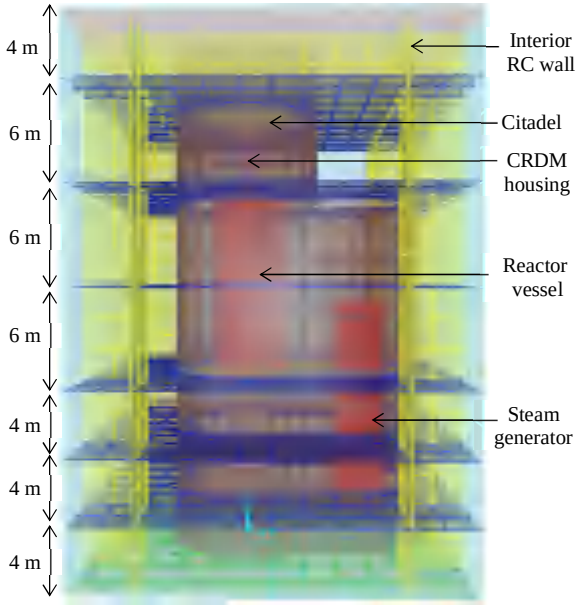

b) elevation view

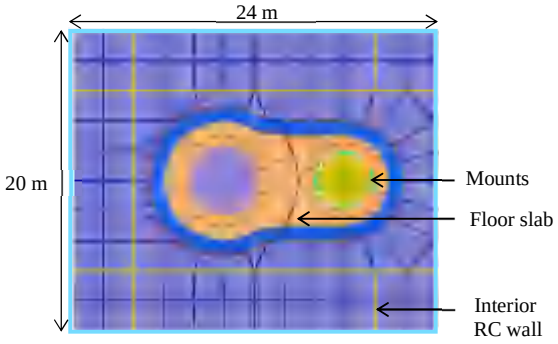

c) plan view at the RV and SG support level

Figure 4. Generic HTGR building

3. Reactor building sites and seismic hazard characterization

Four sets of thirty earthquake ground-motion triplets were developed for nonlinear dynamic analysis of the two reactor buildings. The motions were derived from the seismic hazard studies by Yu ***et al.*** (2018) for the Idaho National Laboratory (INL), in Idaho Falls, ID, and the Los Alamos National Laboratory (LANL) in Los Alamos, NM. The near-surface geology at both sites was assumed to be characterized by a shear velocity of 760 m/s: the boundary between site classes B and C per Standard ASCE/SEI 7-16 (ASCE, 2017a).

Yu ***et al.*** (2018) described horizontal design-basis earthquake (DBE) shaking at the INL and the LANL sites by geomean horizontal acceleration response spectra corresponding to a mean annual frequency of exceedance of 10^{-4} (or return period of 10,000 years), which is the hazard exceedance probability for Seismic Design Category (SDC) 5 per Table 1-2 of ASCE/SEI Standard 43-05 (ASCE, 2005). (Adjustments are required per ASCE 43-05 and ASCE 43-19 to derive a design response spectrum. Consequence analysis might support the use of a lower SDC, with corresponding reductions in the return period of the design shaking. However, neither consideration is applied herein because the outcomes of the study are not affected.) The corresponding design-basis vertical spectra at the two sites were generated by amplitude scaling the horizontal geomean spectra using the ratios of vertical-to-horizontal (V/H) shaking per Figure 7b in Bozorgnia and Campbell (2004) and a controlling source-to-site distance of less than 20 km per the seismic hazard disaggregation described in Yu ***et al***. (2018), namely, 0.9 for frequency equal to 10 Hz and higher, 0.5 for frequency equal to 3.3 Hz and lower, and linear interpolation between 3.3 and 10 Hz. The 10,000-year return period shaking at the INL site has a geomean horizontal peak ground acceleration (PGA) of 0.3 g and a vertical PGA of 0.27 g. The corresponding horizontal and vertical PGAs at the LANL site are 0.5 g and 0.45 g, respectively.

Yu ***et al.*** (2018) generated thirty sets of maximum-minimum ground motion triplets consistent with the target DBE horizontal and vertical spectra at the INL and the LANL sites. (Only the two horizontal components of each triplet were used in Yu's 2018 study.) Four sets of thirty ground-motion triplets were derived from these INL and LANL ground motion studies by amplitude scaling, as identified in Table 1, to represent a wide range of seismic hazard (and possible sites) for a consistent near-surface geology.

Table 1. Seismic hazard characterization

Site (hazard)	Seismic hazard definition	Design PGA	
		Geomean horizontal	Vertical
A (low)	0.5× 10,000-year shaking, INL	0.15 g	0.13 g
B (moderate)	10,000-year shaking, INL	0.30 g	0.27 g
C (high)	10,000-year shaking, LANL	0.50 g	0.45 g
D (very high)	1.4× 10,000-year shaking, LANL	0.70 g	0.63 g

The hazard descriptions in Table 1 enable analysis of the reactor buildings and the equipment for incremented levels of earthquake shaking and investigation of opportunities for standardizing reactor designs using seismic isolation. Figure 5 presents the target geomean horizontal (red solid line) and vertical (blue solid line) acceleration response spectra at sites B and C and acceleration response spectra for the thirty sets (grey solid lines) of horizontal max-min and vertical ground motions.

Varying the near-surface geology (i.e., changing the site class) at a given site (A through D) will affect the shape of the target spectra of Figure 5 and the resultant displacement and force demands in both the buildings and isolation systems, but that is not considered here. Similarly, updating the V/H ratios on the basis of the recent research, which will be included in the 2022 release of ASCE/SEI Standard 7, will affect vertical shaking demands for sites in the Western United States, but those are not considered here either because the effects of vertical shaking, as explained later, are relatively minor for the buildings and equipment considered in this study.

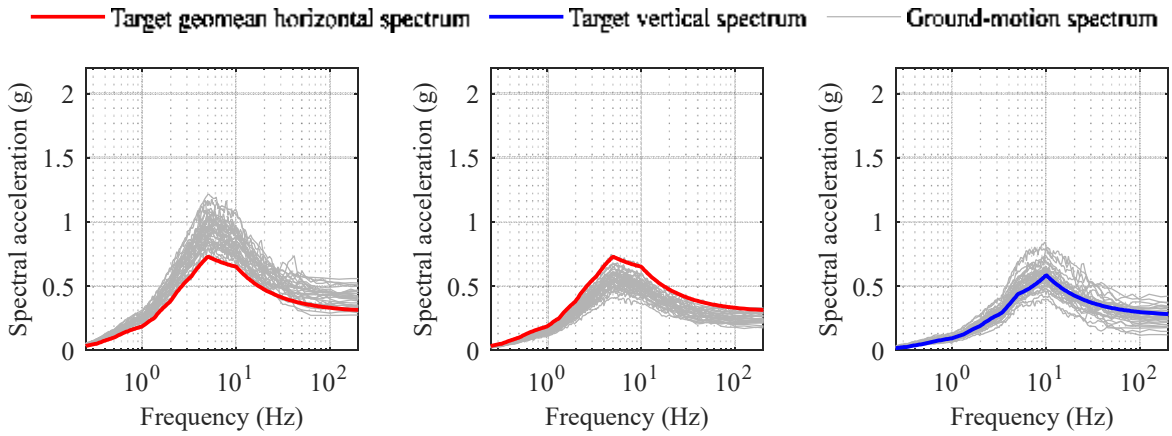

a) horizontal-max, site B b) horizontal-min, site B c) vertical, site B

d) horizontal-max, Site C e) horizontal-min, site C f) vertical, site C

Figure 5. Target spectra and ground motion spectra at sites B and C (Yu *et al.*, 2018)

4. Preliminary design of reactor buildings and safety-class equipment

Preliminary designs for the reactors buildings and the assumed safety-class equipment were developed using ASCE/SEI Standards 4-16 (ASCE 2017a) and 43-05 (ASCE 2005), ACI 349 (ACI, 2013) and the ASME Boiler and Pressure Vessel Code (ASME, 2017). The reactor buildings studied herein have RC structural walls as the vertical elements in the seismic force resisting system. Earthquake shaking affects the thickness and reinforcement in these walls.

To obtain a baseline design for the buildings, the walls were sized by response-spectrum analysis (RSA) using the linearized Regulatory Guide (RG) 1.60 spectrum (USNRC, 2014) amplitude scaled to a horizontal PGA of 0.15 g. Figure 6 enables a comparison between the RG 1.60 spectrum and the target DBE spectrum

at site A. In the frequency range from 0.25 Hz to 25 Hz, and of importance to the reactor buildings and the safety-class equipment considered therein, the RG 1.60 spectrum has higher spectral ordinates than those for site A. In-plane shear stresses in the perimeter RC walls were evaluated for combined gravity and seismic loads and the wall thicknesses were iteratively adjusted till the resulting shear stresses complied with the ***design*** limits of ACI 349. The minimum wall thickness in both buildings was 0.45 m. (The exterior walls and roof slabs should be sufficiently thick to resist wind-borne missile impact).

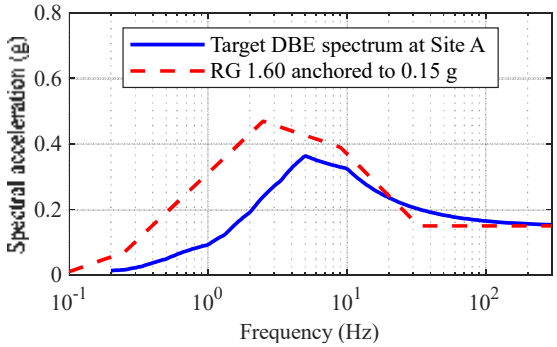

Figure 6. Comparison of RG 1.60 spectrum and horizontal DBE spectrum at Site A

The authors worked with subject matter experts at TerraPower (MSR) and X-energy (HTGR) to identify and select representative geometries, material properties, reactive mass of vessel internals, boundary conditions, and a range of operating conditions (temperature, internal pressure, service life) for the reactor vessels (RV) and steam generators (SG), denoted hereafter as RV_{MSR}, SG_{MSR}, RV_{HTGR}, and SG_{HTGR}. All four vessels were designed as Class 1 components. Because many advanced reactors are being designed to operate at elevated temperatures (e.g., Goldberg and Rosner (2011), Kinsey and Jessup (2018)), material design strengths must account for the effects of long-term service at high temperatures. The design of Class I pressure boundary components for elevated temperature service (>425^{o}C) must comply with the requirements of Section III, Division V of the ASME code. At lower operating temperatures, Section III, Division I of the ASME code can be used.

The four vessels were sized initially for operational loads only, which are expected throughout normal operation of the reactor, and classed by ASME as service level A. Membrane stress intensity demands from internal pressure and gravity were checked against service level A limits to obtain minimum wall thickness in each vessel. To indirectly address local bending stresses and other loadings, the minimum wall thickness was increased by incrementing the operating pressure by 20%. The assumed operating conditions and material alloy for each vessel are presented in Table 2. Although HTGRs operate at very high temperatures, the temperature of its primary coolant in contact with the vessel is expected to range between 250°C and 350°C, and so an intermediate value of 285°C was assumed herein for design. Because the operating pressure in a MSR (5 to 10 bars) is much smaller than that in a HTGR (60 bars), the MSR vessel walls, for operational loadings, are much thinner than those of the HTGR.

Table 2. Operational design of the safety-class vessels: assumptions

Parameter	MSR		HTGR	
	Reactor vessel	Steam generator	Reactor vessel	Steam generator
Operating temperature (°C)	500	500	285	285
Material	SS316	SS316	SA508	SA516
Stress intensity limit[1] (MPa)	106	106	184	114
Operating internal pressure (bar)	5	10	60	60
Inner diameter of the vessel (m)	5	3	4.5	3.5
Operational wall thickness (mm)	15	20	85	104

[1]Service level A limit per HBB-3223 for the MSR vessels and per NBB-3223 for the HTGR vessels

5. Numerical modeling and response-history analysis

Numerical models for the two baseline reactor buildings (designed for RG 1.60 spectrum, 0.15 g PGA) coupled with the safety-class equipment (designed for operational loads only) were developed in SAP2000 (CSI, 2019). The total weight of the baseline MSR (HTGR) building, including equipment, is approximately 55,000 (11,500) tons. The reactor and steam generator vessels, roof slabs, floor slabs, buttresses, basemat, citadel walls, and interior and exterior RC walls in the buildings were modeled using four-node shell elements. The CRDM housings were modeled as beam elements with appropriate cross-sectional properties. A mesh sensitivity study was performed to determine the optimal mesh size for each component.

Concrete was assumed to be uncracked with a uniaxial compressive strength of 40 MPa. The density, Poisson's ratio, and modulus of elasticity of concrete were assumed as 2400 kg/m^3, 0.2, and 30 GPa, respectively. The material modulus of elasticity for the pressure vessels was adjusted for the operating temperature: RV_{MSR} = 170 GPa (SS 316 at 500°C), SG_{MSR} = 170 GPa (SS 316 at 500°C), RV_{HTGR} = 175 GPa (SA 508 at 285°C), and SG_{HTGR} = 185 GPa (SA 516 at 285°C). The density and Poisson's ratio of all three steel alloys were assumed to be 7850 kg/m^3 and 0.3, respectively. The reactive mass of the RV internals, including a fraction of mass of reactor fuel/coolant, neutron reflectors, core barrel, and other internal equipment laterally braced to the vessel, was assumed to be 300 tons (250 tons) for the MSR (HTGR). A reactor head supports components internal and external to the vessel and so representative masses were lumped on the head in each building. The reactive mass of the SG_{MSR} and SG_{HTGR} internals were assumed to be 200 tons and 150 tons, respectively, and were attached to the walls of the vessels. Representative masses were added to the tops and bottoms of the steam generators to account for external attachments, including steam and feedwater plenums. Table 3 presents the modal frequencies of the baseline reactor buildings and the equipment. In the vertical direction, the mass participation in the equipment was distributed across several modes, and coupled with the vertical modes of the supporting floor slabs, and hence well-defined vertical frequencies for the equipment could not be identified.

Table 3. Horizontal modal frequencies of the buildings and the equipment

	MSR	HTGR
Building	7 to 8 Hz	5 to 6 Hz
Reactor vessel	11 Hz	8 Hz
Steam generator	7 Hz	13 Hz
CRDM housing	22 Hz	18 Hz

The fast-nonlinear analysis solver in SAP2000 was used to perform response-history analyses (RHA) for the thirty ground-motion triplets at each site. The max-min components of the horizontal shaking were randomly oriented along the principal axes of the building.

Soil-structure interaction was neglected because a) near-surface geology was not characterized beyond site class per ASCE/SEI 7, and b) the effects were anticipated to be negligible for the horizontally flexible, base-isolated buildings. Best-estimate mechanical properties were assumed to model the structural framing.

The basemat nodes were restrained to simulate conventional (non-isolated) construction. For the MSR (HTGR), the first 150 (100) Ritz modes recovered 99% and 90% of the mass in the horizontal and the vertical directions, respectively, and were used for the response-history analyses. Modal damping of 4% was assumed in both buildings. Although 4% damping is reasonable for the reinforced concrete buildings, it is too high for the steel safety-class equipment, for which 2% (or less) damping would be appropriate. However, the modal responses of the SG_{MSR} and RV_{HTGR} are coupled with the building response and it was not possible to separately assign damping to the reinforced concrete components and the steel equipment. Seismic demands (stresses and accelerations) in the equipment were calculated at the 80th percentile non-exceedance probability (per ASCE 4, but addressing ground-motion variability only) and then increased by 25% to adjust for the 2% (or less) damping.

Equipment designed for operational loadings (service level A) per the ASME Boiler and Pressure Vessel code will have some capacity to resist the effects of earthquake shaking (service levels C or D), in large part because higher stress intensities are permitted. For shaking beyond a threshold intensity, the thickness of the walls of the vessels must be increased to resist earthquake-induced loadings. Stresses were monitored near, but not at points of support of the vessels and compared with the ASME service level C stress intensity limits. Wall thickness was increased in 2-mm increments, and the analysis repeated, until the resulting stress intensity complied with the ASME limits. Acceleration histories along the heights of vessels, and at points of attachment and at cantilever tips of CRDM housings were monitored, as identified by green solid circles in Figure 7. Locations #a1 and #b1 are points of attachment of equipment; #a2, #a4, #a5, #b2, #b4, and #b5 are representative locations for vessel internals; and #a3 and #b3 are the tips of the CRDM housings. Peak accelerations at locations #a2, #a3, #a4, #a5, #b2, #b3, #b4, and #b5 were calculated at the 80th percentile and increased by 25% to account for the 2% (or less) damping in steel safety-class equipment.

6. Impact of the seismic load case on equipment design and RC wall thickness

Table 4 presents vessel weights as a function of site horizontal PGA, normalized by the value required for operational loadings (=100 units). The seismic penalty, as evident in the table, is significant, ranging from a 20% to 130% increase in weight for site D (PGA = 0.7 g). The percentage increase at site D for the SG_{HTGR}

is small, in large part because the vessel is supported at two-thirds its height and because of its larger thickness for operational loadings.

Table 4. Normalized vessel weights in the fixed-base buildings

	RV_{MSR}	SG_{MSR}	RV_{HTGR}	SG_{HTGR}
Operational	100	100	100	100
Site A (0.15 g)	107	110	104	100
Site B (0.30 g)	133	135	120	103
Site C (0.50 g)	160	185	142	109
Site D (0.70 g)	187	230	167	120

Table 5 presents peak geomean horizontal accelerations in the safety-class equipment. For site D, the acceleration at the bottom of the RV_{MSR} is 2.50 g, an amplification of approximately four from the PGA. Greater amplifications are observed in the HTGR building, in part, because equipment is supported on a suspended floor slab and input motion is amplified by building response to location #b1. The peak acceleration of 9.6 g (13 g) at the tip of the CRDM housing in the HTGR building at site C (D) is a 19-fold increase on PGA, and is a consequence of building and equipment first mode frequencies being similar. (Such accelerations would likely trigger redesign of the housing and the reactor head.)

Consideration of the earthquake load case increases the thickness (and reinforcement) of the RC walls and slabs in the buildings. Only the walls are addressed herein. The thickness of the walls was iteratively adjusted upwards, in increments of 25 mm, until the resulting shear stresses complied with the ***design*** limits of the ACI 349. (High shear stresses in the walls will require dense reinforcement and complex detailing, contributing substantially to construction time and cost.) Table 6 presents the required thickness of the perimeter RC walls as a function of increasing earthquake shaking. The trial wall thickness of 0.45 m is sufficient to resist earthquake shaking at site A for both the MSR and HTGR buildings. The required wall thickness increases for both buildings at the three sites with PGA greater than 0.15 g, and by a factor of approximately three for shaking at Site D.

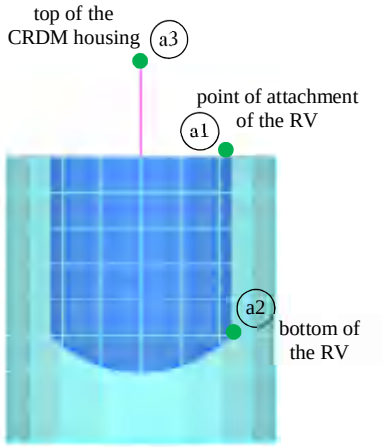

a) RV assembly, MSR

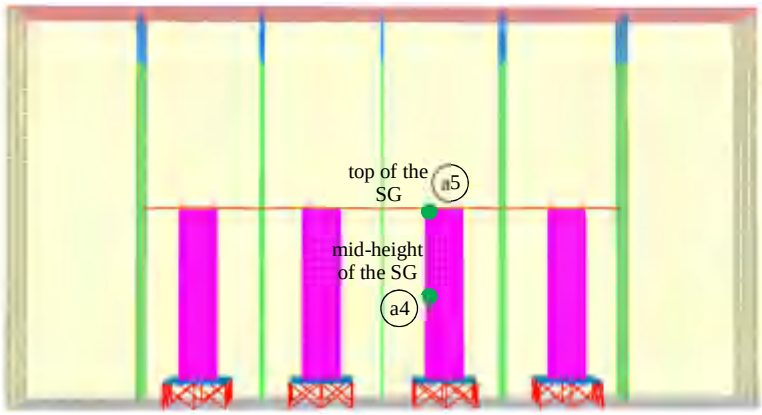

b) SG assembly, MSR

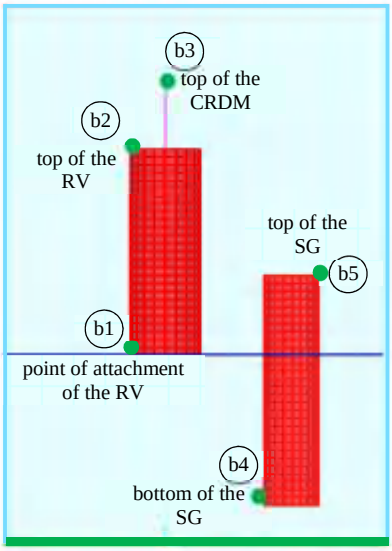

c) RV and SG assembly, HTGR

Figure 7. Locations of interest for the safety-class equipment for acceleration response

Table 5. Equipment horizontal accelerations (g)

	Response location		Site (PGA)			
			A (0.15 g)	B (0.3 g)	C (0.5 g)	D (0.7 g)
MSR	PoA of the RV_{MSR}	#a1	0.24	0.47	0.74	1.1
	Bottom of the RV_{MSR}	#a2	0.67	1.3	1.8	2.5
	Top of the $CRDM_{MSR}$	#a3	1.1	2.0	3.1	3.8
	Mid-height the SG_{MSR}	#a4	0.75	1.4	2.2	3.1
	Top of the SG_{MSR}	#a5	1.1	2.3	3.6	5.0
HTGR	PoA of the RV_{HTGR}	#b1	0.32	0.66	1.0	1.4
	Top of the RV_{HTGR}	#b2	1.4	3.0	5.3	7.5
	Top of the $CRDM_{HTGR}$	#b3	3.1	5.7	9.6	13
	Top of the SG_{HTGR}	#b4	0.58	1.2	1.8	2.4
	Bottom of the SG_{HTGR}	#b5	0.75	1.4	2.1	2.9

Table 6. Thickness of the perimeter RC walls as a function of site

Earthquake intensity	MSR[1] building		HTGR[2] building	
	x-direction	*y*-direction	*x*-direction	*y*-direction
Site A (0.15 g)	0.45	0.45	0.45	0.45
Site B (0.30 g)	0.60	0.60	0.60	0.60
Site C (0.50 g)	0.90	0.90	0.75	1.0
Site D (0.70 g)	1.2	1.2	1.0	1.4

[1] *x*- and *y*-direction are walls along the 90 m and 60 m direction, respectively

[2] *x*- and *y*-direction are walls along the 24 m and 20 m direction, respectively

7. Seismic isolation of reactor buildings

The next release of ASCE/SEI Standard 4 will recognize an expanded set of seismic isolation and damping devices, including low damping rubber bearings, lead-rubber bearings, spherical sliding (or Friction Pendulum) bearings, spring-based bearings, uniaxial fluid viscous dampers, and 3D pot dampers. The spring-based bearings and 3D pot dampers enable vertical and 3D isolation. The other bearings enable 2D (horizontal) isolation, which is the focus of this study. Figure 1b identifies these isolators and dampers.

The fixed-base reactor buildings and equipment designed for site A were considered as the baseline models for designing 2D horizontal seismic isolation systems at the other three sites. Figure 8 shows the assumed isolation system layout for the MSR and the HTGR buildings, consisting of 124 and 30 bearings, respectively. They are denoted by [tag, bearing type, site]: [#IS1, single concave Friction Pendulum (SFP) bearings, site B]; [#IS2, Lead-rubber (LR) bearings, site C]; [#IS3, Triple Friction Pendulum (TFP) bearings, site D]. A different isolator type was considered for each site, but the layout and the number of isolators were not altered. The bearing properties are presented in Tables 7, 8, and 9 for SFP, LR, and TFP bearings, respectively. The SAP2000 program includes materials, namely, '*Friction isolator*', '*Rubber isolator'*, and '*Triple Friction Isolator'* which can simulate nonlinear hysteretic behavior of SFP, LR, and TFP bearings, respectively, although without the advanced features identified in Kumar *et al.* (2019a;

2019b), and Sarlis and Constantinou (2013). For this study, the vertical stiffness of the isolators was assumed to be very high. (In practice, isolator geometry would be sized, vertical stiffness calculated, and modeled explicitly.) The isolators were modeled as two-node link elements. Nonlinear response-history analyses were performed for the isolated buildings with the isolator links as the only nonlinear components. Results are presented in Figures 9, 10, and 11, and Tables 10 and 11.

As shown in Figure 9, the seismic penalty on vessel weight in the base-isolated (BI) buildings is negligible, and smaller than those for the fixed-base (FB) buildings at sites B, C, and D. For the PGA = 0.7 g site, vessel weights are reduced from 187 to 107 for the RV_{MSR}, from 230 to 110 for the SG_{MSR}, and from 167 to 104 for the RV_{HTGR}. Similarly, the RC walls in both buildings, sized for PGA = 0.15 g shaking, are sufficient for site D if base isolation is implemented. At site D, base isolation led to significant reductions in the peak horizontal accelerations in the equipment, by factors of between 2 and 13, from their fixed-base counterparts, as shown in Figure 10 and Table 10. Spectral demands for the equipment in the fixed-base buildings at site A are generally greater those in the base-isolated buildings at sites B, C, and D, but seismic qualification of equipment in the standardized buildings at the four sites would utilize enveloping spectra.

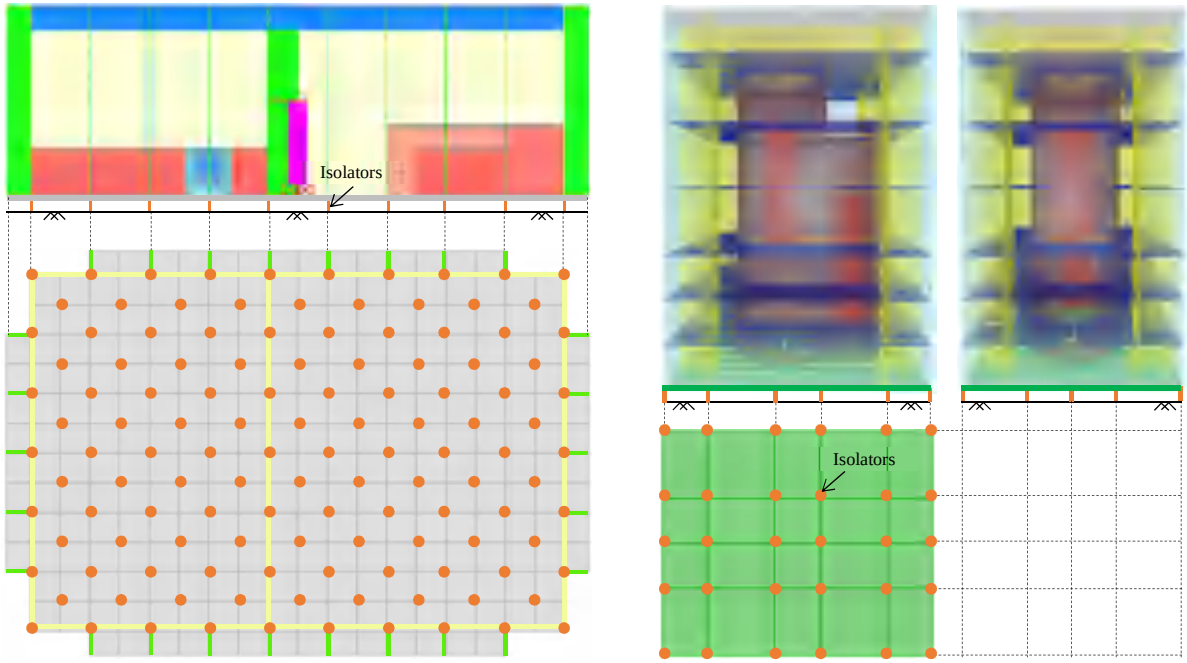

a) MSR building b) HTGR building

Figure 8. Layout of the building-level isolation systems

Table 7. Site B isolation system properties – SFP bearings (#IS1)

Parameter	Units	MSR	HTGR
Fast coefficient of friction	-	0.05	0.05
Slow coefficient of friction	-	0.025	0.025
Radius of curvature of the sliding surface	mm	2240	2240
Rate parameter	sec/mm	0.1	0.1
Sliding period	sec	3	3

Table 8. Site C isolation system properties – LR bearings (#IS2)

Parameter	Units	MSR	HTGR
Outer diameter of the bearing	mm	750	750
Diameter of the lead core	mm	200	200
Thickness of each rubber layer (steel shim)	mm	9 (3)	9 (3)
Number of rubber layers (steel shims)	-	25 (24)	25 (24)
Yield stress of lead	MPa	10.5	10.5
Shear modulus of rubber	MPa	0.8	0.8
Bulk modulus of rubber	MPa	2000	2000
Total yield strength/Gravity load	-	0.08	0.09
Post-elastic period	sec	3.5	3.24

Table 9. Site D isolation system properties – TFP bearings (#IS3)

Parameter	Units	MSR	HTGR
Fast coefficient of friction at the outer (inner) sliding surfaces	-	0.10 (0.02)	0.10 (0.02)
Slow coefficient of friction at the outer (inner) sliding surfaces	-	0.05 (0.01)	0.05 (0.01)
Radius of curvature of the outer (inner) sliding surfaces	mm	2240 (300)	2240 (300)
Rate parameter at all four sliding surfaces	sec/mm	0.1	0.1
Sliding period (on the outer surfaces)	sec	4.24	4.24

Table 10. Geomean horizontal accelerations (g) in the fixed-base and isolated buildings

	Response location		Fixed-base	Building-isolated		
			Site A	Site B	Site C	Site D
MSR	PoA of the RV_{MSR}	#a1	0.24	0.10	0.12	0.20
	Bottom of the RV_{MSR}	#a2	0.67	0.54	0.24	0.64
	Top of the $CRDM_{MSR}$	#a3	1.1	0.37	0.27	0.79
	Mid-height of the SG_{MSR}	#a4	0.74	0.25	0.46	0.57
	Top of the SG_{MSR}	#a5	1.1	0.25	0.50	0.44
HTGR	PoA of the RV_{HTGR}	#b1	0.32	0.12	0.14	0.29
	Top of the RV_{HTGR}	#b2	1.4	0.38	0.38	0.58
	Top of the $CRDM_{HTGR}$	#b3	3.1	1.1	0.59	2.7
	Top of the SG_{HTGR}	#b4	0.58	0.30	0.21	0.84*
	Bottom of the SG_{HTGR}	#b5	0.75	0.68	0.42	1.4*

* Isolation-system properties could be optimized to reduce this acceleration.

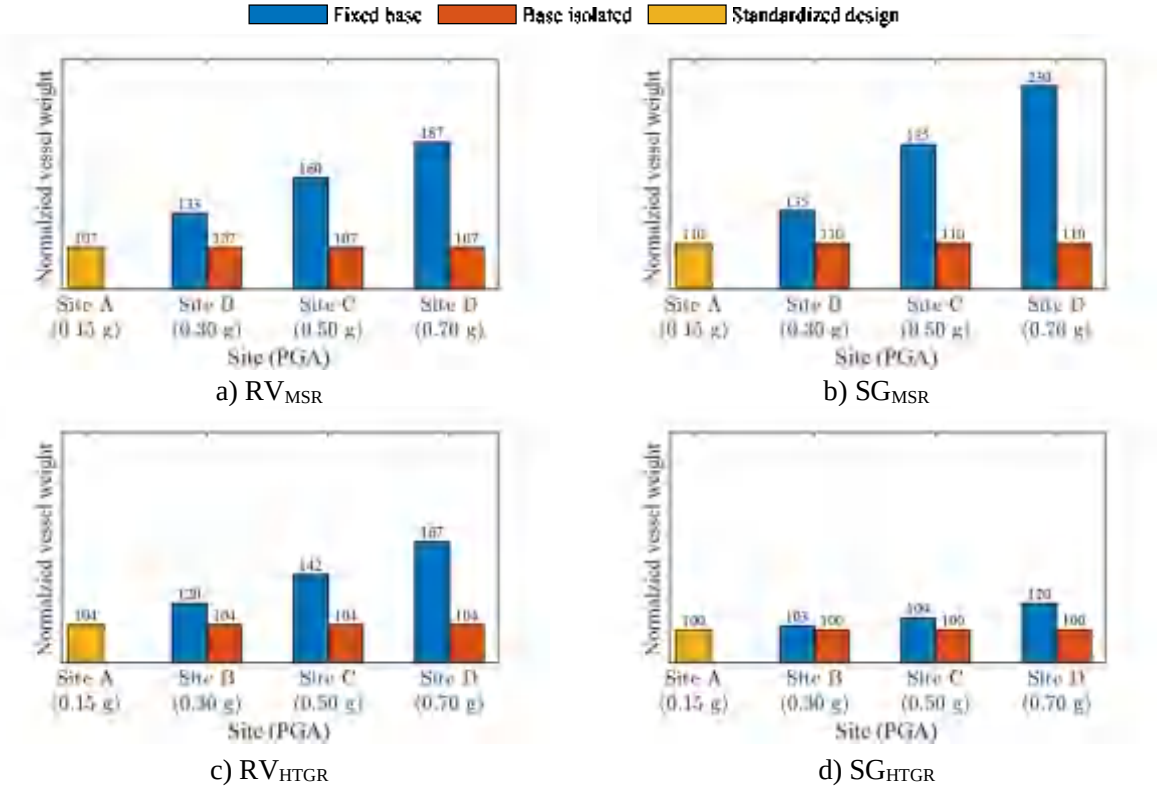

a) RV_{MSR} b) SG_{MSR}

c) RV_{HTGR} d) SG_{HTGR}

Figure 9. Normalized vessel weights in the isolated buildings

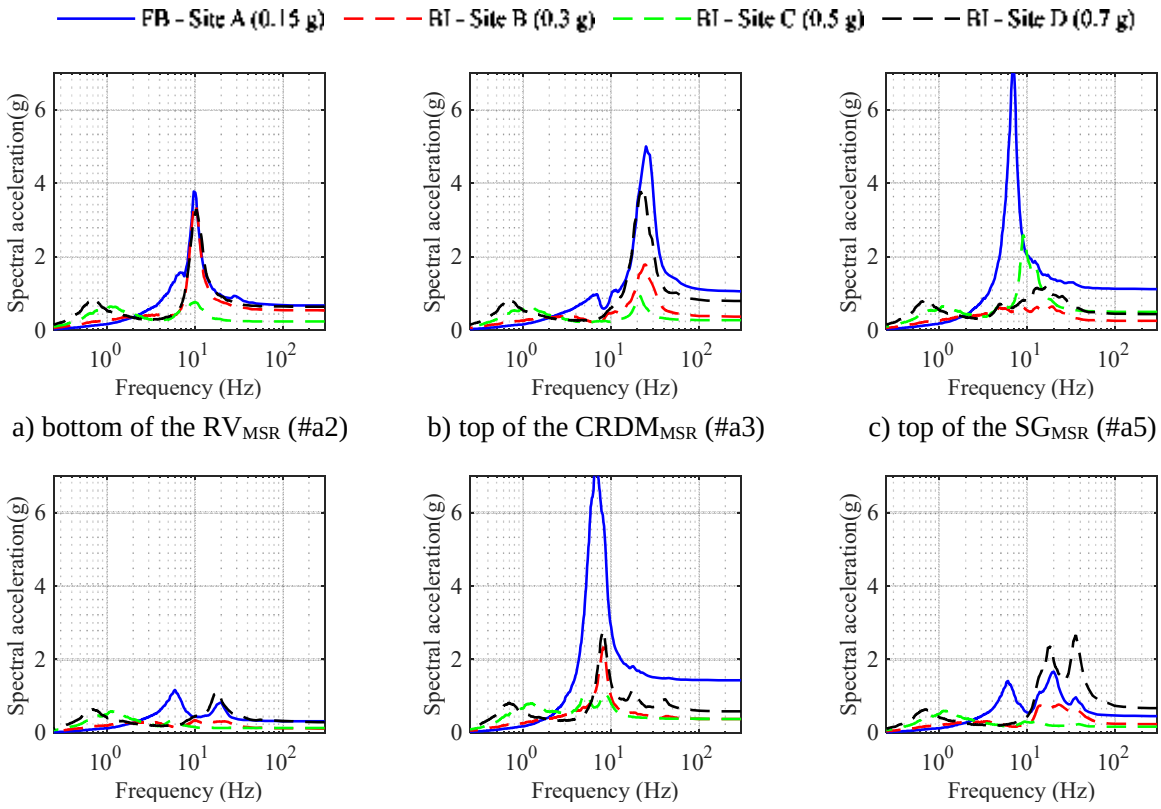

a) bottom of the RV_{MSR} (#a2) b) top of the $CRDM_{MSR}$ (#a3) c) top of the SG_{MSR} (#a5)

d) PoA of the RV_{HTGR} (#b1) e) PoA of the $CRDM_{MSR}$ (#b2) f) top of the SG_{HTGR} (#b4)

Figure 10. 5% damped geomean horizontal acceleration spectra in the isolated buildings

Peak SRSS isolator displacements are reported in Table 11. All can be easily accommodated by the isolators of Tables 7, 8, and 9. Safety-related umbilical lines (e.g., piping) crossing the isolation interface would have to be designed and qualified to accommodate these displacements. Additional displacement capacity in the isolators and umbilical lines may be needed to achieve plant-level safety goals but site- and reactor-specific seismic probabilistic risk assessment (SPRA) is beyond the scope of this paper.

Table 11. Peak SRSS isolator displacements (mm), building isolation

Building	Site B (#IS1)	Site C (#IS2)	Site D (#IS3)
MSR	70	145	245
HTGR	71	137	243

The results presented above make clear that identical reactor buildings and equipment designed for a site of low seismic hazard (PGA = 0.15 g) can be deployed at sites of much higher seismic hazard, up to 0.70 g PGA here, without modification, if the buildings are base-isolated: a pathway to standardization and drastic reductions in capital cost (Lal *et al.*, 2021). Only the isolation system, substructure, and safety-critical umbilical lines crossing the isolation interface would need to be analyzed, designed, and qualified for a new site (based on site-specific hazard analysis and geotechnical investigations) to limit seismic demands (stresses, accelerations, and displacements) in the building and equipment to previously qualified capacities. In practice, the properties (or type) of an isolation system and the umbilical lines may not need to be changed for every new site. For example, an isolation system and umbilical lines designed for a PGA = 0.4 g site

could be deployed at a PGA = 0.3 g site, without modification, for similar or identical near-surface geology, substantially descoping the required engineering and the associated cost.

The isolation systems considered for the analysis above will attenuate only the horizontal components of ground motion. Because vertical inputs are not attenuated, the effects of increasing vertical shaking from site A to site D must be addressed for standardized reactor installation if only 2D (horizontal) isolation systems are implemented. For the buildings and equipment studied herein, the effects of increased vertical shaking are smaller than those for horizontal shaking, in part because gravity loading is a design consideration for operational loadings and there is margin for increased vertical acceleration. In Figure 9, although the vertical shaking is increased from site A to site D, the vessel weights in the isolated buildings remain constant showing little to no effect of vertical shaking.

Vertical acceleration could affect the design and qualification of equipment attached to the reactor and steam generator. See Figure 11, which presents the amplification (from the input PGA) in peak vertical acceleration in the equipment at site D. In the fixed-base buildings, vertical acceleration is amplified by between 2 and 4, and much smaller than the amplification in the horizontal direction (between 2 and 19). The vertical amplification in the isolated buildings is similar to that in the fixed-base buildings because the isolation systems considered herein are assumed to be axially rigid. For standardized designs, isolated building framing and equipment must be designed and qualified for vertical shaking not attenuated and perhaps amplified by 2D (horizontal) isolators, unless vertical isolation is also implemented (IAEA, 2020b; Nawrotzki *et al.*, 2019).

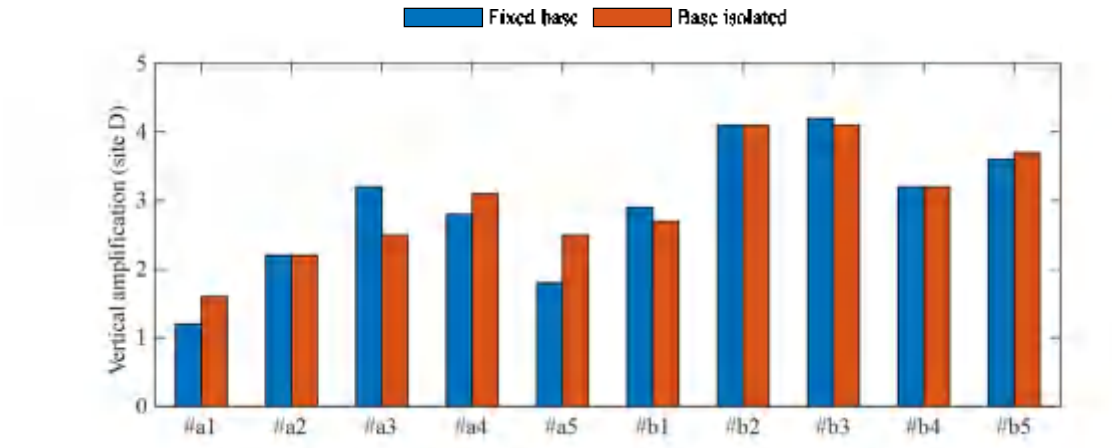

Figure 11. Amplification of Site D vertical acceleration in the fixed-base and isolated buildings

8. Summary, key outcomes, and closing remarks

The seismic load case challenges the standardization of advanced nuclear reactors, which is likely a necessary step for their widespread commercial deployment. For conventionally founded reactor buildings, site-specific seismic hazard and near-surface geology obliges soil-structure interaction analysis, design, equipment qualification, regulatory review, and licensing. Mitigating the impact of the seismic load case enables standardization of advanced reactors (the building and equipment contained within the green-dashed rectangle of Figure 1a), substantially reducing the scope of the pre-construction design-related activities and driving down construction cost.

Characterizing the impact of the seismic load case on the design of two fundamentally different advanced reactor buildings and six generic pieces of safety-class equipment was a focus of this paper. A range of geometries, material properties, reactive masses, boundary conditions, and equipment operating conditions were assumed for each piece of equipment and *generic* designs were developed following ASCE and ACI practice for the buildings and ASME practice for the equipment. Numerical models were developed and analyzed for four intensities of earthquake shaking, and fixed-base and base-isolated configurations. The isolation systems were not optimized, not all available isolation and damping systems were considered, and only one site class (or near-surface geology) was studied. Because the reactor buildings and the equipment studied in this paper are not specific to one reactor developer, the trends presented below are considered applicable to other advanced reactor types, buildings, and equipment, and spectral shapes and amplitudes other than those of Figure 5, including those more representative of earthquake shaking in the Central and Eastern United States:

- The seismic penalty on the weight of the reactor vessels and the steam generators installed in the fixed-base buildings can be significant. To meet ASME design requirements, the thickness of the walls of the reactor vessel (steam generator) must be increased from the value sufficient for operational loadings (=100) to 187 (230) in the example MSR building and to 167 (120) units in the example HTGR building for site D (PGA = 0.7 g). The increase in thickness will impact the design and layout of other safety-class equipment (e.g., reactor vessel auxiliary cooling systems), anchorages, and structural framing.
- The seismic penalty on equipment can be greatly reduced by base isolating the reactor building. For the example MSR and HTGR, a 10% (or less) increase in the weights of the reactor vessels and steam generator vessel, from that required for operational performance, would provide sufficient seismic capacity to resist earthquake shaking of PGA = 0.7 g (site D) if the buildings are base isolated. The peak horizontal accelerations in the equipment considered here are reduced by a factor between 2 and 13 if base isolation is implemented.
- The RC walls in both example buildings, sized assuming conventional (non-isolated) construction and a PGA = 0.15 g site, are sufficient to resist shaking approximately five times as intense if base isolation is deployed, reducing the volume of nuclear grade concrete in the walls by a factor of approximately 2 for the buildings and sites considered herein.
- Base isolation enables re-use of reactor building designs, including safety-class equipment. As demonstrated for the example MSR and HTGR, buildings and equipment designed assuming conventional (i.e., non-isolated) construction for a low seismicity site (e.g., site A) can be constructed at sites of higher seismic hazard (e.g., sites B, C, and D) by selecting an appropriate seismic isolation system, as demonstrated in this paper.

Kammerer ***et al.*** (2016) identified regulatory challenges and gaps related to licensing seismically isolated advanced reactors. Figure 4 in that report introduces a site-independent, certified design, which in essence is the licensed standardized reactor building enclosed by the green-dashed rectangle in Figure 1a. The site-independent, certified design would be characterized by horizontal and vertical acceleration response spectra, consistent with Subpart B of 10 CFR 52, defined at the underside of the basemat and immediately above the isolation system of Figure 1a. Site-specific engineering (analysis, design, regulatory review, licensing, and qualification) would be limited in scope to the substructure below the standardized plant (i.e., the isolators, pedestals, and foundation in Figure 1a) with the primary goal of demonstrating that the chosen isolation system limits the design-basis shaking demands to the limiting values associated with the certified

design. Qualification of safety-class equipment would be limited to prototype and production testing of the seismic isolators and/or damping devices, and safety-related umbilical lines crossing the isolation interface.

Section 3.2 of Kammerer *et al.* (2016) identifies one of the challenges associated with site-independent, certified design supported by a seismic isolation system, namely, vertical shaking effects that are not attenuated by long period, 2D seismic isolation systems capable of large horizontal displacements (e.g., the spherical sliding, lead-rubber, and low-damping rubber bearings, and uniaxial fluid viscous damper of Figure 1a). In this paper, vertical shaking was addressed using the ratios of vertical-to-horizontal shaking of Bozorgnia and Campbell (2004). Probabilistic seismic hazard analysis, which is mandated for a new build nuclear power plant in the United States, will include site-specific values for the ratio, which might be greater or less than those adopted for this study.

Site-specific SPRA will be needed for isolated (and non-isolated) advanced reactors. Standardization and seismic isolation should simplify these calculations for both Part 52 and Part 53 licensing. Work is underway at the time of this writing to develop SPRA procedures for base-isolated advanced reactors.

As noted in this paper, a seismic penalty, albeit small, will be paid for a seismically isolated, standardized advanced reactor. A challenge is to determine the optimal seismic robustness of a standardized plant, in terms of horizontal and vertical acceleration response spectra defined at the underside of the basemat. A starting point is to determine the seismic capacity of the reactor's safety-class equipment designed for operational loadings only, which was adopted in this paper. A next step is to define a seismic design category per ASCE 43, and a family of possible sites, soil classes, V/H ratios, and 2D and 3D isolation solutions, to limit horizontal and vertical shaking demands to the seismic capacity of the certified reactor building. Iterations with techno-economic feedback will be needed to develop optimal solutions, sufficient for deployment at scale.

Acknowledgements

The information, data, and work presented herein was funded by the U.S. Department of Energy under CRADA 17TCF10, by the Electric Power Research Institute under Agreement MA 10008959, and the Advanced Research Project Agency-Energy (ARPA-E) under Award Number DE-AR0000978. The views and opinions of the authors expressed herein do not necessarily state or reflect those of United States Government or any agency thereof. The authors thank Mr. Michael Cohen (TerraPower) and Mr. Paul Kirchman (X-energy) for advising the authors on the mechanical design of the vessels.

References

American Concrete Institute (ACI). (2013). "Code requirements for nuclear safety-related concrete structures and commentary." *ACI 349-13*, Farmington Hills, MI.

American Society of Civil Engineers (ASCE). (2005). "Seismic design criteria for structures, systems, and components in nuclear facilities." *ASCE/SEI 43-05*, Reston VA.

American Society of Civil Engineers (ASCE). (2017a). "Minimum design loads for buildings and other structures." *ASCE/SEI 7-16*, Reston VA.

American Society of Civil Engineers (ASCE). (2017b). "Seismic analysis of safety-related nuclear structures and commentary." *ASCE/SEI 4-16*, Reston VA.

American Society of Civil Engineers (ASCE). (2021). "Seismic design criteria for structures, systems, and components in nuclear facilities." *ASCE/SEI 43-19*, Reston VA.

American Society of Mechanical Engineers (ASME). (2017). "ASME Boiler and Pressure Vessel Code." New York, NY.

Bolisetti, C., Yu, C.-C., Coleman, J. L., Kosbab, B., and Whittaker, A. S. (2016). "Characterizing the benefits of seismic isolation for nuclear structures: a framework for risk-based decision making." *INL/EXT-16-40122*, Idaho National Laboratory, Idaho Falls, ID.

Bozorgnia, Y., and Campbell, K. W. (2004). "The vertical-to-horizontal response spectral ratio and tentative procedures for developing simplified V/H and vertical design spectra." *Journal of Earthquake Engineering*, 8(2), 175-207.

Buongiorno, J., Corradini, M., Parsons, J., and Petti, D. (2018). "The future of nuclear energy in a carbon constrained world - an interdisciplinary MIT study." *MIT Energy Initiative*, Massachusetts Institute of Technology, Cambridge, MA.

Computers and Structures Inc (CSI). (2019). Computer Program SAP2000 (Version 20.1), Berkeley, CA.

Energy Technologies Institute (ETI). (2020). "The ETI nuclear cost drivers project: Full technical report." Loughborough, UK.

Goldberg, S., M., and Rosner, R. (2011). "Nuclear reactors: Generation to generation." *American Academy of Arts and Sciences*, ISBN#: 0-87724-090-6.

Huang, Y.-N., Whittaker, A. S., and Luco, N. (2008). "Performance assessment of conventional and base-isolated nuclear power plants for earthquake and blast loadings." *Technical Report MCEER-08-0019*, University at Buffalo, The State University of New York, Buffalo, NY.

Huang, Y.-N., Whittaker, A. S., Kennedy, R. P., and Mayes, R. L. (2009). "Assessment of base-isolated nuclear structures for design and beyond-design basis earthquake shaking." *Technical Report MCEER-09-0008*, University at Buffalo, The State University of New York, Buffalo, NY.

Huang, Y.-N., Whittaker, A. S., and Luco, N. (2011a). "A seismic risk assessment procedure for nuclear power plants: (I) Methodology." *Nuclear Engineering and Design*, 241, 3996-4003.

Huang, Y.-N., Whittaker, A. S., and Luco, N. (2011b). "A seismic risk assessment procedure for nuclear power plants: (II) Application." *Nuclear Engineering and Design*, 241, 4004-4011.

International Atomic Energy Agency (IAEA). (2020a). "Driving deeper decarbonization with nuclear energy." *IAEA Bulletin, Volume 61-3*, Vienna, Austria.

International Atomic Energy Agency (IAEA). (2020b). "Seismic isolation systems for nuclear installations." *IAEA-TECDOC-1905*, Vienna, Austria.

Ingersoll, E. D., and Gogan, K. (2020). "Missing link to a livable climate: How hydrogen-enabled synthetic fuels can help deliver the Paris goals." LucidCatalyst, Cambridge, MA.

Ingersoll, E. D., Gogan, K., Herter, J., and Foss, A. (2020). "Cost and performance requirements for flexible advanced nuclear plants in future U.S. power markets." LucidCatalyst, Cambridge, MA.

Kammerer, A., Whittaker, A. S., and Coleman, J. L. (2016). "Proposed activities to address regulatory gaps and challenges for licensing advanced reactors using seismic isolation." *Technical Report INL/EXT-16-40668*, Idaho National Laboratory, Idaho Falls, ID.

Kammerer, A. M., Whittaker, A. S., and Constantinou, M. C. (2019). "Technical considerations for seismic isolation of nuclear facilities." *NUREG/CR-7253*, United States Nuclear Regulatory Commission, Washington, D.C. (ML19050A422).

Kinsey, S., and Jessup, W. (2018). "United States nuclear manufacturing infrastructure assessment." *DOE-MPRA-NE000638*, USDOE Office of Nuclear Energy.

Kumar, M., Whittaker, A. S., and Constantinou, M. C. (2017a). "Extreme earthquake response of nuclear power plants isolated using sliding bearings." *Nuclear Engineering and Design*, 316, 9-25.

Kumar, M., Whittaker, A. S., Kennedy, R. P., Johnson, J. J., and Kammerer, A. (2017b). "Seismic probabilistic risk assessment for seismically isolated safety-related nuclear facilities." *Nuclear Engineering and Design*, 313, 386-400.

Kumar, M., Whittaker, A. S., and Constantinou, M. C. (2019a). "Seismic isolation of nuclear power plants using sliding bearings." *NUREG/CR-7254*, United States Nuclear Regulatory Commision, Washington, D.C. (ML19158A513).

Kumar, M., Whittaker, A. S., and Constantinou, M. C. (2019b). "Seismic isolation of nuclear power plants using elastomeric bearings." *NUREG/CR-7255*, United States Nuclear Regulatory Commision, Washington, D.C. (ML19063A541).

Lal, K. M., Parsi, S. S., and Whittaker, A. S. (2020). "Cost basis for utilizing seismic isolation for nuclear power plant design." *Report 03002018345*, Electric Power Research Institute, Charlotte, N.C.

Lal, K. M., Parsi, S. S., Kosbab, B. D., Ingersoll, E. D., Charkas, H., and Whittaker, A. S. (2021). "Towards standardized advanced nuclear reactors: Seismic isolation and the impact of the earthquake load case." *Nuclear Engineering and Design*, (under review).

Nawrotzki, P., Siepe, D., and Salcedo, V. (2019). "Seismic protection of NPP structures using 3-D base control systems." *Transactions: 25th International Conference on Structural Mechanics in Reactor Technology (SMiRT-25)*, Charlotte, NC.

Sarlis, A. A., and Constantinou, M. C. (2013). "Model of triple friction pendulum bearing for general geometric and frictional parameters and for uplift conditions." *Technical Report MCEER-13-0010*, University at Buffalo, State University of New York, Buffalo, NY.

Tajirian, F. F., Kelly, J. M., and Gluekler, E. L. (1989). "Testing of seismic isolation bearings for the PRISM advanced liquid metal reactor under extreme loads." *Transactions: 10th International Conference on Structural Mechanics in Reactor Technology (SMiRT-10)*, Anaheim, CA.

Tajirian, F. F. (1992). "Seismic analysis for the ALMR." *Proceedings: International Atomic Energy Agency (IAES) Specialists' Meeting on Seismic Isolation Technology*, San Jose, CA.

Tajirian, F. F., and Patel, M. R. (1993). "Response of seismic isolated facilities: a parametric study of the ALMR." *Transactions: 12th International Conference on Structural Mechanics in Reactor Technology (SMiRT-12)*, Stuttgart, Germany.

United States Nuclear Regulatory Commission (USNRC). (2014). "Design response spectra for seismic design of nuclear power plants." *Regulatory Guide 1.60*, Washington, D.C.

Whittaker, A. S., Sollogoub, P., and Kim, M. K. (2018). "Seismic isolation of nuclear structures: Past, present, and future." *Nuclear Engineering and Design*, 338, 290-299.

Yu, C.-C., Bolisetti, C., Coleman, J. L., Kosbab, B., and Whittaker, A. S. (2018). "Using seismic isolation to reduce risk and capital costs of safety-related nuclear facilities." *Nuclear Engineering and Design*, 326, 268-284.

Appendix A. Equipment-level seismic isolation

An alternative implementation of seismic isolation is considered in this appendix, namely, to isolate structures, systems, components, and safety-class equipment inside a nuclear facility. This deployment would allow for standardized design of equipment, and should eliminate the need for its site-specific analysis, design, and qualification, although it cannot likely achieve cost reductions approaching those possible with building-level isolation. Equipment isolation may be a financially attractive solution for those reactor buildings that are deeply embedded, for which building-level isolation is impractical.

In this appendix, horizontal (2D) isolation solutions are presented for the six pieces of safety-class equipment considered in the body of the paper. Three dimensional isolation systems are possible but not pursued here. In the MSR building, the RV is isolated using four LR bearings installed between the reactor head and a surrounding cylindrical RC shield structure, as shown in Figure A1a. Each steam generator was isolated at its mid-height using three equally-spaced support mounts. The isolators were installed beneath the support mounts and atop a steel frame as shown in Figure A1b. In the HTGR building, the floor slab supporting the RV and SG (shown in orange in the plan view of Figure A1c) is supported on eleven isolators, each installed on a reinforced concrete pedestal extending up from the basemat. In both buildings, clearance is provided around the equipment to allow unrestricted horizontal movement of the isolation system. Possible elevated temperatures and radiation exposure, which would be design considerations in practice, were neglected for this study.

To illustrate a process, a different 2D isolation system was selected for each piece of equipment and identified by [tag, equipment, type, properties]: [#EIS1, RV_{MSR}, 4 LR bearings, Table A1]; [#EIS2, SG_{MSR}, 3 SFP bearings each, Table A2]; [#EIS3, Equipment floor slab HTGR, 11 TFP bearings, Table A3]. For convenience, the same isolation system was deployed at sites B, C, and D for this introductory study.

The dynamic analyses performed for the build-level isolations systems of Section 7 were repeated using the ground motion triplets of Section 3. Peak horizontal accelerations in the equipment calculated at the 80th percentile are reported in Table A4. Equipment designed for the fixed-base (conventional) condition at site A could be deployed, by-and-large, at sites B, C, and D if seismically isolated, enabling standardization, noting that the isolation solutions adopted herein were not optimized. Peak horizontal accelerations are reduced by a factor of between 3 and 12 in the MSR building and between 4 and 7 in the HTGR building for site D if the seismic isolation solutions assumed here are deployed.

Table A5 presents peak isolator displacements, calculated at the 80th percentile, for the three sites and isolated equipment. Safety-critical umbilical lines crossing the isolation interface would have to be designed and qualified to accommodate these displacements, noting that isolator stability is not challenged here. Isolators and safety-related umbilical lines crossing the isolation interface will likely have to accommodate displacements greater than the values of Table A5 to achieve safety goals but site-specific SPRA is beyond the scope of this paper, as noted previously.

The analysis results presented above make clear that seismic isolation is a viable pathway to standardized equipment in advanced reactors. For equipment, an optimal isolation system will be a trade-off between reduced acceleration demands in the equipment and displacements across the isolation interface, which will require reactor-specific analysis, fragility studies, and risk calculations.

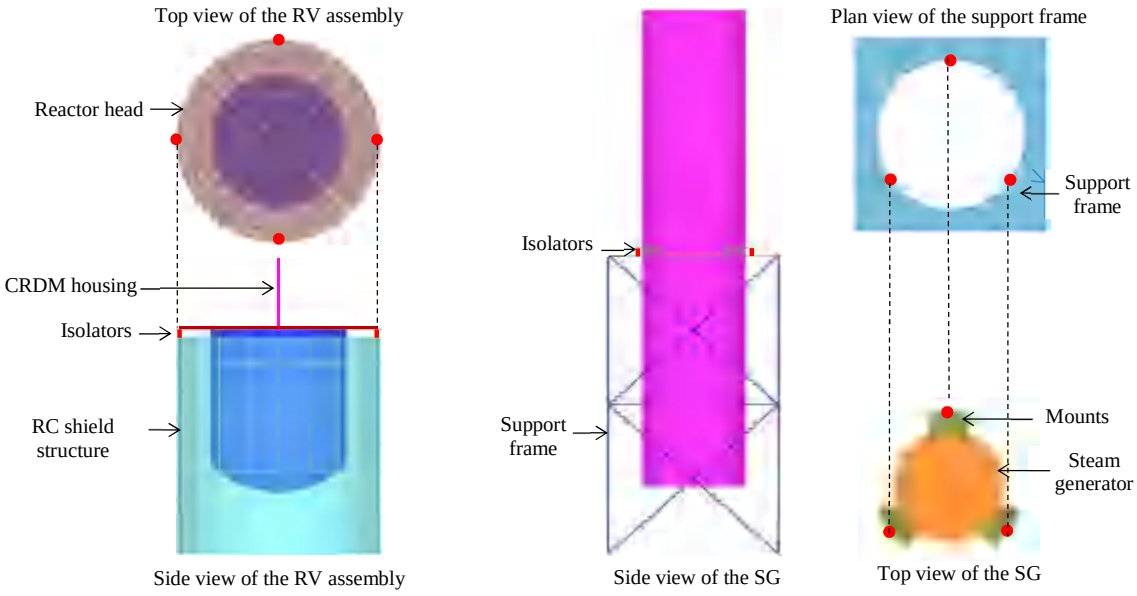

a) isolated RV assembly, MSR

b) isolated SG, MSR

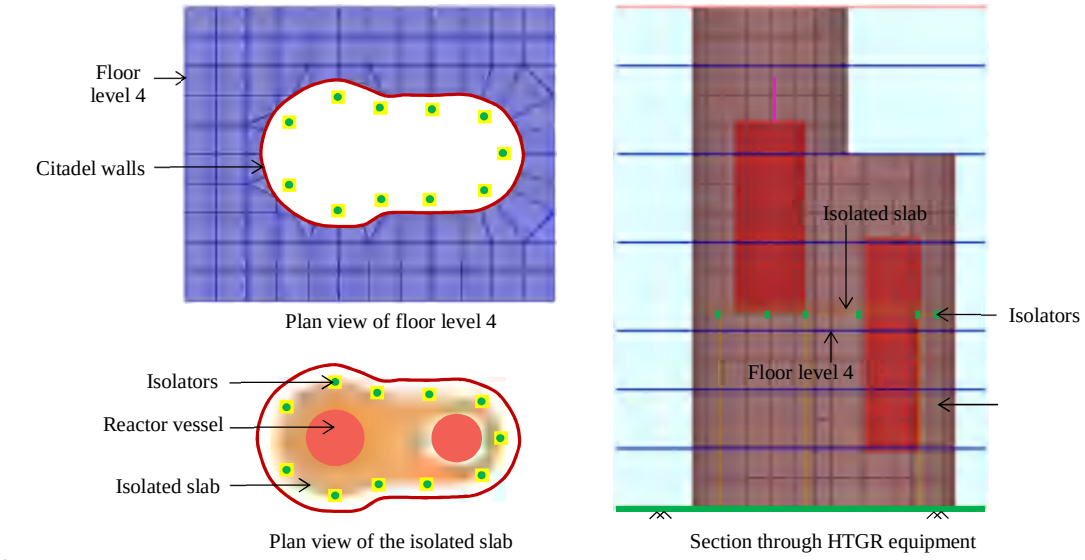

,

c) isolated equipment, HTGR

Figure A1. Isolation system layout for the safety-class equipment

Table A1. Isolation system properties for RV_{MSR} – LR bearings (#EIS1)

Parameter	Units	Value
Outer diameter of the bearing	mm	650
Diameter of the lead core	mm	150
Thickness of each rubber layer (steel shim)	mm	9 (3)
Number of rubber layers (steel shims)	-	25 (24)
Yield stress of lead	MPa	10.5
Shear modulus of rubber	MPa	0.8
Bulk modulus of rubber	MPa	2000
Total yield strength/Gravity load	-	0.19
Post-elastic period	sec	2

Table A2. Isolation system properties for SG_{MSR} – SFP bearings (#EIS2)

Parameter	Units	Value
Fast coefficient of friction	-	0.12
Slow coefficient of friction	-	0.06
Radius of curvature of the sliding surface	mm	1550
Rate parameter	sec/mm	0.1
Sliding period	sec	2.5

Table A3. Isolation system properties for $Floor_{HTGR}$ – TFP bearings (#EIS3)

Parameter	Units	Value
Fast coefficient of friction at the outer (inner) sliding surfaces	-	0.10 (0.02)
Slow coefficient of friction at the outer (inner) sliding surfaces	-	0.05 (0.01)
Radius of curvature of the outer (inner) sliding surfaces	mm	1550 (300)
Rate parameter at all four sliding surfaces	sec/mm	0.1
Sliding period (on the outer surfaces)	sec	3.5

Table A4. Peak geomean horizontal accelerations (g), equipment isolation

Response location			Fixed-base	Equipment-isolated		
			Site A	Site B	Site C	Site D
MSR	PoA, RV	#a1	0.24	0.19	0.24	0.30
	Bottom, RV	#a2	0.67	0.24	0.32	0.38
	Top, CRDM	#a3	1.1	0.29	0.39	0.51
	Mid-height, SG	#a4	0.74	0.22	0.28	0.35
	Top, SG	#a5	1.1	0.25	0.32	0.43
HTGR	PoA, RV	#b1	0.32	0.21	0.29	0.40
	Top, RV	#b2	1.4	0.52	0.84	1.2
	Top, CRDM	#b3	3.1	1.2	2.0	2.8
	Top, SG	#b4	0.58	0.31	0.45	0.60
	Bottom, SG	#b5	0.75	0.44	0.65	0.87

Table A5. Peak SRSS isolator displacements (mm), equipment isolation

Isolation system	Site B (0.3 g)	Site C (0.5 g)	Site D (0.7 g)
RV_{MSR} (#EIS1)	43	91	148
SG_{MSR} (#EIS2)	29	73	139
$Floor_{HTGR}$ (#EIS3)	93	164	231